

Two-dimensional Tissue Image Reconstruction Based on Magnetic Field Data

Jarmila DĚDKOVÁ, Ksenia OSTANINA

Dept. of Theoretical and Experimental Electrical Engineering, Brno University of Technology, Kolejní 2906/4,
612 00 Brno, Czech Republic

dedkova@feec.vutbr.cz, xostan00@stud.feec.vutbr.cz

Abstract. *This paper introduces new possibilities within two-dimensional reconstruction of internal conductivity distribution. A new algorithm for the conductivity reconstruction was developed. This algorithm utilizes the internal current information with respect to corresponding boundary conditions and the induced magnetic field measured outside the object. A series of computer simulations has been conducted to assess the performance of the proposed algorithm within the process of estimating electrical conductivity changes in the lungs, heart, and brain tissues captured in two-dimensional piecewise homogeneous chest and head models. The reconstructed conductivity distribution using the proposed method is compared with that using a conventional method based on Electrical Impedance Tomography (EIT). The acquired experience is discussed and the direction of further research is proposed.*

Keywords

Impedance tomography, magnetic resonance, image reconstruction, inverse problem, finite element method.

1. Introduction

An image reconstruction technique based on impedance tomography has been an active research topic since the early 1980s. Since this time, there have been significant efforts to produce cross-sectional images of impedivity (conductivity and permittivity) distribution inside the human body using boundary measurements of current-voltage data. This technique is commonly called Electrical Impedance Tomography [1]. An interesting overview of different possibilities within general tomography techniques and their recent applications can be found in [2], [3].

Based on many other published studies, it is possible to say that medical imaging has been one of the prominent applications of EIT. Biological tissues have different electrical properties that change with cell concentration, cellular structure and density, molecular composition, membrane characteristics, and other factors. Consequently, the

properties reflect structural, functional and pathological conditions of the tissue and can provide valuable diagnostic information. Many researchers have tested out the electrical conductivity of tissues and shown that there is a difference in conductivity between a normal and a fatigued tissue and between a healthy and a pathologic tissue [4]. In [5], the author has used the degree of resistance of the brain tissue to an electric current as a means of differentiating between the normal brain and a tumor tissue on the operating table. The conductivity of normal tissues has been measured experimentally; other details can be found e.g. in [6-8]. Further, we will focus on conductivity only since it constitutes an important physical index that can indicate conditions of tissues or organs.

In recent years, numerous studies have attempted to develop algorithms which reconstruct cross-sectional conductivity images from Magnetic Resonance Electrical Impedance Tomography (MREIT) [9-12]. The question of using the MREIT for recovering the interior object conductivity σ when the current is applied on its boundary is very often discussed. The injecting currents produce a magnetic field which has been used together with measured voltage-current data for recovering the conductivity distribution. While the EIT suffers from the ill-posed nature of the corresponding inverse problem, the MREIT has been presented as a conductivity imaging modality providing images with better spatial resolution and accuracy. Unfortunately, by injecting current through surface electrodes we measure only one component of the induced internal magnetic flux density using an MRI scanner. In order to reconstruct the conductivity distribution inside the imaging object, most algorithms in the MREIT have required multiple magnetic flux density data during the injection of at least two independent currents [13].

In this paper, one direct method for reconstructing the internal isotropic conductivity is proposed; it is necessary to know only one component of magnetic flux density data when injecting one current into the imaging object through a single pair of surface electrodes. Firstly, the proposed method reconstructs the density of a projected current, which is a uniquely determined current from the measured one component of the magnetic flux density outside the imaging object. Using the relation between the electric

field and the current density, based on Ohm’s law, the additional condition can be introduced to an implicit matrix system for the determination of internal conductivity distribution.

Here, the described techniques utilize internal information on the induced magnetic field in addition to the boundary current-voltage measurements to produce images of internal current density and conductivity distributions. In this paper, a new way to obtain these distributions without the knowledge of voltage data on the boundary of the proposed testing object is presented. It is shown that this technique can be applied conveniently to identify the location of regions with different conductivity values or to identify local changes of these values.

2. Basic Theory

The current density \mathbf{J} in a linear medium with the interior electrical conductivity σ can be obtained from the electric field \mathbf{E} or the corresponding potential distribution U

$$\mathbf{J} = \sigma \cdot \mathbf{E} = -\sigma \cdot \text{grad}U . \tag{1}$$

The impedance tomography problem is a recovery of the conductivity distribution satisfying the continuity equation

$$\text{div} \mathbf{J} = 0 .$$

Now we consider the two-dimensional numerical model with N_E linear triangle elements with N_U nodes (see e.g. Fig. 1). We approximate (1) from nodal values U_i using linear approximation functions $N_i(x, y)$ on a grid of linear triangular finite elements

$$U(x, y) \approx \sum_{i=1}^{N_U} U_i \cdot N_i(x, y) . \tag{2}$$

Then we can describe the current density $\mathbf{J}^{(e)}(x, y)$ on each element (e) by (3)

$$\mathbf{J}^{(e)}(x, y) \approx -\sigma^{(e)} \sum_{j=1}^3 U_j^{(e)} \text{grad}N_j^{(e)}(x, y) \tag{3}$$

where $\sigma^{(e)}$ and $N_j^{(e)}(x, y)$ are the conductivity and the linear approximation function on element (e). We now consider that the current is injected into a two-dimensional electrically conductive object. The induced magnetic flux density \mathbf{B} corresponding to \mathbf{J} can be described using the Biot-Savart law. If the magnetic flux density \mathbf{B} due to the injection current is known from the measurements, an image of the corresponding internal current density distribution \mathbf{J} can be obtained from, for example, Ampere’s law

$$\mathbf{J} = \text{rot} \mathbf{B} / \mu_0 .$$

This method naturally requires the knowledge of all components of a magnetic field; therefore, in the following text, we will propose a simpler procedure. The magnetic

field \mathbf{B}_i can be calculated numerically in the general point given by coordinates $[x_i, y_i, z_i]$ using the Biot-Savart law and the principle of superposition

$$\mathbf{B}_i \approx \frac{\mu_0}{4\pi} \sum_{j=1}^{N_E} \frac{\mathbf{J}_j \times \mathbf{R}_{ij}}{R_{ij}^3} \Delta V_j \tag{4}$$

where N_E is the number of elements, \mathbf{J}_j is the current density on element j , ΔV_j represents the volume of element j , and \mathbf{R}_{ij} represents the distance between the centre $[x_j, y_j, z_j]$ of element j and the point $[x_i, y_i, z_i]$. The components of magnetic field can be expressed

$$B_{xij} = \frac{\mu_0}{4\pi} \frac{J_{yj} R_{zij} \Delta V_j}{R_{ij}^3}, \quad B_{yij} = -\frac{\mu_0}{4\pi} \frac{J_{xj} R_{zij} \Delta V_j}{R_{ij}^3},$$

$$B_{zij} = \frac{\mu_0}{4\pi} \cdot \frac{(J_{xj} R_{yij} - J_{yj} R_{xij}) \Delta V_j}{R_{ij}^3} .$$

It is obvious that, to obtain the N_E pair of J_x and J_y components of a current density, we have to know either the same number of B_x and B_y components or the double number of B_z component of a magnetic field. Let us suppose we know the $2 N_E$ values of B_z ; then, each of them is given

$$B_{zi} = \sum_{j=1}^{N_E} (K_{Ryij} J_{xj} + K_{Rxij} J_{yj}) , \quad i = 1, \dots, 2N_E .$$

The matrix notation of $2N_E$ algebraic equations is

$$\begin{bmatrix} \mathbf{K}_{Ry} & \mathbf{K}_{Rx} \end{bmatrix} \cdot \begin{bmatrix} \mathbf{J}_x \\ \mathbf{J}_y \end{bmatrix} = \mathbf{B}_z \Leftrightarrow \mathbf{K}_R \cdot \mathbf{J} = \mathbf{B} . \tag{5}$$

From (5) we can obtain the source current density distribution very easily

$$\mathbf{J} = \mathbf{K}_R^{-1} \cdot \mathbf{B} . \tag{6}$$

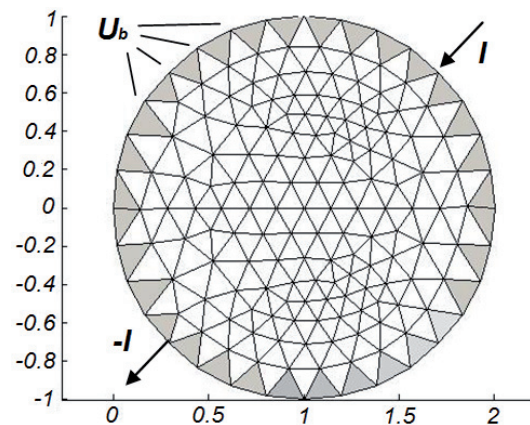


Fig. 1. An arrangement for numerical simulations.

The conductivity reconstruction process is usually presented as the minimization of the primal objective function $\mathcal{Y}_U(\sigma)$, which can be based on the Method of Least Squares and the Tikhonov regularization method [1]

$$\Psi_U(\sigma) = \frac{1}{2} \sum \|\Delta U\|^2 + \frac{1}{2} \alpha \|\mathbf{L}\sigma\|^2, \Delta U = U_M - U_{FEMb}(\sigma). \quad (7)$$

Here, U_M , U_{FEMb} are the measured and calculated voltages on the object boundary, α is a regularization parameter, \mathbf{L} is a suitable regularization matrix, σ is the unknown vector of conductivity distribution inside the object. After applying the Newton-Raphson method, the iteration procedure can be obtained

$$\sigma_{i+1} = \sigma_i + (\mathbf{J}_i^T \mathbf{J}_i + \alpha \mathbf{L}^T \mathbf{L})^{-1} (\mathbf{J}_i^T \Delta U_i - \alpha \mathbf{L}^T \mathbf{L} \sigma_i).$$

Here, i is the i -th iteration and \mathbf{J} is the Jacobian

$$\mathbf{J}_i = \frac{\partial U_{FEMb}(\sigma)}{\partial \sigma}.$$

This way we look for such conductivity distribution which minimizes the difference between the measured and calculated voltages on the boundary U_M , U_{FEMb} . The size of U_M depends on the number of measuring electrodes and the number of current patterns.

However, the above-described solution is not the only one possible. We can also minimize the difference between current densities \mathbf{J}_M and \mathbf{J}_{FEM} on the elements. The \mathbf{J}_{FEM} vector corresponds to calculated voltage U_{FEM} and it can be computed using U_{FEM} and (3). The \mathbf{J}_M vector can be obtained from the measured value of magnetic field using (6). Then, the object function $\Psi_K(\sigma)$ can be described

$$\Psi_K(\sigma) = \frac{1}{2} \sum \|\Delta \mathbf{J}\|^2 + \frac{1}{2} \alpha \|\mathbf{L}\sigma\|^2, \Delta \mathbf{J} = \mathbf{J}_M - \mathbf{J}_{FEM}(\sigma). \quad (8)$$

The meaning of parameters α and \mathbf{L} is the same as that mentioned above. If we apply the Newton-Raphson method, we obtain the iteration procedure

$$\sigma_{i+1} = \sigma_i + (\mathbf{J}_i^T \mathbf{J}_i + \alpha \mathbf{L}^T \mathbf{L})^{-1} (\mathbf{J}_i^T \Delta \mathbf{J}_i - \alpha \mathbf{L}^T \mathbf{L} \sigma_i).$$

Here, i is the i -th iteration and \mathbf{J}_i is the corresponding Jacobian

$$\mathbf{J}_i = \frac{\partial \mathbf{J}_{FEM}(\sigma)}{\partial \sigma} = \begin{bmatrix} \frac{\partial \mathbf{J}_{FEM1}}{\partial \sigma_1}, & \frac{\partial \mathbf{J}_{FEM1}}{\partial \sigma_2}, & \dots & \frac{\partial \mathbf{J}_{FEM1}}{\partial \sigma_{N_E}} \\ \vdots & \vdots & & \vdots \\ \frac{\partial \mathbf{J}_{FEMN_E}}{\partial \sigma_1}, & \frac{\partial \mathbf{J}_{FEMN_E}}{\partial \sigma_2}, & \dots & \frac{\partial \mathbf{J}_{FEMN_E}}{\partial \sigma_{N_E}} \end{bmatrix}.$$

In the following part, an example is shown of the magnetic field distribution, the corresponding surface current density distribution, and the influence of nonhomogeneity inside the tested sample. From the difference of current density \mathbf{J} in the samples without nonhomogeneity and with nonhomogeneity, we can obtain the conductivity distribution using the conditions on the boundary between two media with different conductivities. The forward solution system equation can be described using the Finite Element

Method

$$\mathbf{K}(\sigma) \mathbf{U}_{FEM}(\sigma) = \mathbf{F}.$$

The forward operator \mathbf{U}_{FEM}

$$\mathbf{U}_{FEM}(\sigma) = \mathbf{K}^{-1}(\sigma) \mathbf{F}$$

can be calculated more effectively if we know the conductivities on all boundary elements. In this case, we can recalculate very easily, using (3), the potential U_b at the corresponding N_b boundary nodes, see Fig. 1. This means that the number of equations N_U for the forward solution can be reduced to $(N_U - N_b)$ equations and that we can save the computational time.

3. Numerical Simulations

The basic arrangements of the average conductivity distribution of healthy tissues in the slice of a chest and a head can be seen in Fig. 2 ($N_E = 300$, $N_U = 167$) and Fig. 3 ($N_E = 2360$, $N_U = 1237$). The finite element mesh for each simulation model was created by using program Ansys 12.0; then regions representing the different types of biological tissues were chosen. The chest model has 20 cm diameter. The width of head model is 14.40 cm and its height is 19.95 cm.

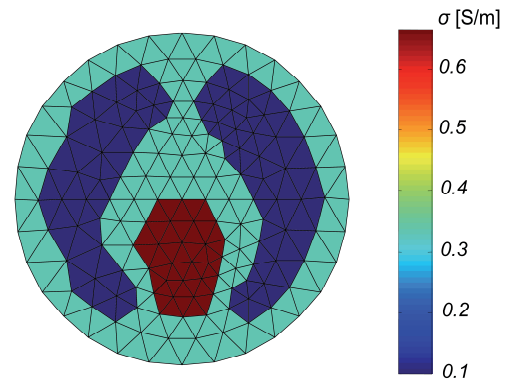


Fig. 2. A chest model for the reconstruction of conductivity changes in heart or lungs.

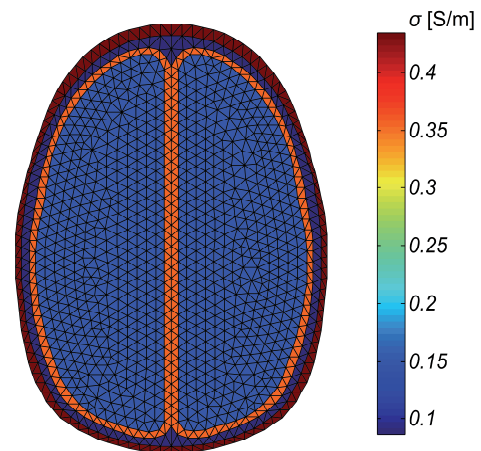


Fig. 3. A head model for the reconstructions of conductivity changes.

In Fig. 2, the simplified model represents the chest with just three homogeneous isotropic layers: lung (dark blue color), heart (brown color) and body tissue (blue color). The next simulation model presented in Fig. 3 is a simplified model of the human head, which consists of four homogeneous isotropic layers: gray and white matters (orange and blue colors), the skull (dark blue color), and the scalp (brown color). Therefore, it is necessary to know only values of average regional conductivities of chest tissues and head tissues of corresponding models for realization of image reconstruction.

The knowledge and the easy monitoring of tissue conductivity changes are very useful and crucial in clinical medicine for diagnostics and during the therapy. The conductivity values of different biological tissues used for the following simulations are presented in Tab. 1; these values were taken from previously published literature on this topic, see [14].

Tissue	Conductivity [S/m]
Heart	0.667
Lung	0.100
Body tissue	0.333
Gray matter	0.352
White matter	0.147
Skull	0.087
Scalp	0.435
Blood	0.900
Blood clot	0.300
Tumor	0.956

Tab. 1. The electrical conductivity of human tissues.

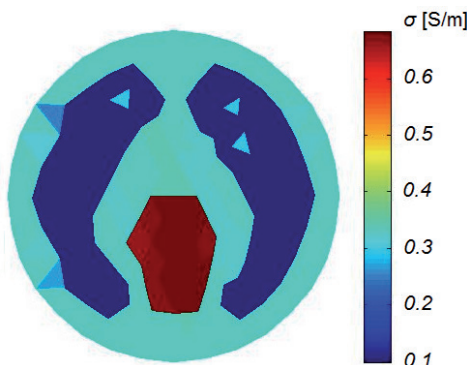


Fig. 4. The detection of blood clots in lungs.

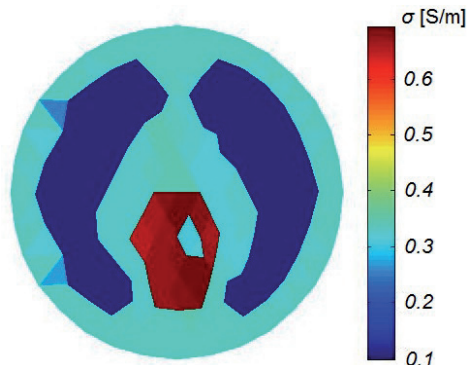


Fig. 5. The detection of a blood clot in a heart.

The first reconstruction results of conductivity changes detection are presented in the Fig. 4 and 5. The final conductivity image with the detection of blood clot regions in lungs is shown in Fig. 4; original blood clot regions are represented by three triangle elements inside lungs with conductivity 0.3 S/m.

The result in Fig. 5 demonstrates the detection of a blood clot in a heart; in this case the original blood clot region is represented by three elements inside a heart with conductivity 0.3 S/m.

It is well known that the conductivity of a tumor tissue is significantly greater than that of a normal tissue. The conductivity imaging techniques could be potentially useful also for early diagnosis of tumors. However, in order to visualize any tumor at its early stage, the reconstructed conductivity image must be accurate with a high spatial resolution of any arbitrary tumor size and locations.

Fig. 6 presents two different reconstruction results related to the detection of several small brain tumors. The original brain tumor distribution is represented by six elements with conductivity 0.956 S/m. In the figure, the left section shows the final conductivity distribution when the object function Ψ_U given by (7) was optimized (old way), and the right section contains the same result when the Ψ_K given by (8) was optimized (new way). The behavior of both object functions during the iteration process is shown in Fig. 7.

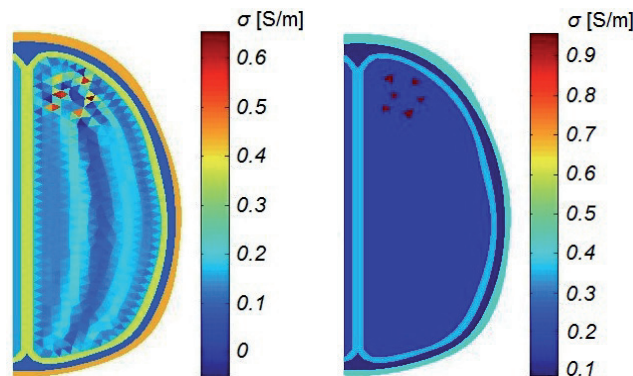


Fig. 6. The detection of tumors in the brain (Ψ_U used on the left, Ψ_K on the right).

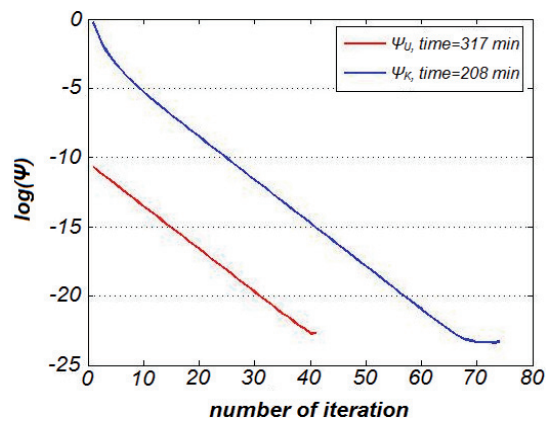


Fig. 7. Objective functions during the detection of tumors.

The next example shows another possible method of brain tumors detection. In this case, the filter reducing the number of unknowns was introduced to both tested algorithms. Fig. 8 presents a comparison between results obtained through a reconstruction based on the Ψ_U optimization (left) and results achieved by means of the Ψ_K optimization (right). The behavior of object functions Ψ_U and Ψ_K is, during the reconstruction, similar to the description shown in Fig. 7. The algorithm run time was in both cases significantly reduced by the application of a suitable filter during the reconstruction process [15]; it was reduced three times for an old algorithm and fifteen times for a proposed algorithm.

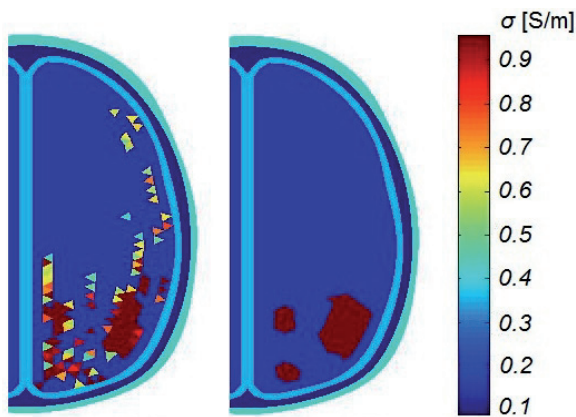


Fig. 8. The detection of three brain tumors (Ψ_U used on the left, Ψ_K on the right).

The last example demonstrates the applicability of the new algorithm for detection of brain blood clot. In this case, the defect represents the simplified model of blood clot. Fig. 9 presents a comparison between results obtained through a reconstruction based on the Ψ_U optimization (left) and results achieved by means of the Ψ_K optimization (right). In Fig. 10, the object functions Ψ_U and Ψ_K are compared during the reconstruction. All obtained reconstruction results show that the proposed algorithm stably and reliably determines the conductivity changes in an imaging slice.

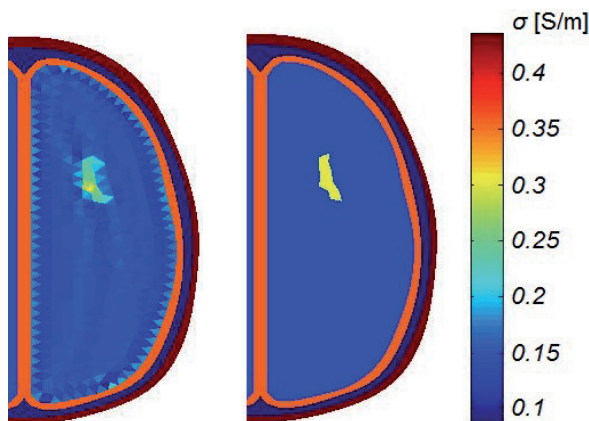


Fig. 9. The detection of a blood clot in the brain (Ψ_U used on the left, Ψ_K on the right).

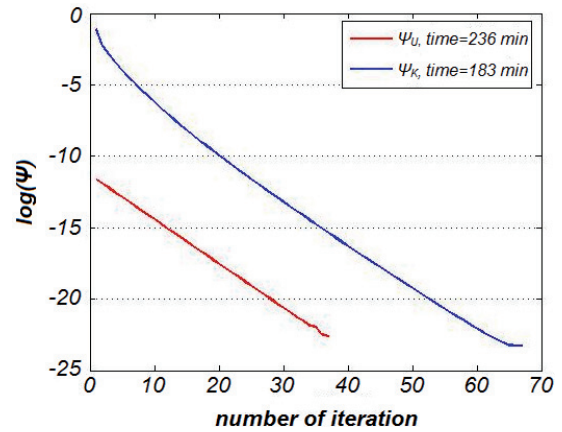


Fig. 10. Objective functions during the detection of a blood clot.

All above-presented simulations were obtained under the condition that the size of \mathbf{U}_M was 380 and size of \mathbf{J}_M was 789.

The high degree of accuracy was achieved by applying the new algorithm, namely the same conductivity distribution as original ones was obtained as a result of imaging by this algorithm in all these cases.

4. Conclusion

A new approach to the two-dimensional reconstruction of conductivity distribution based on using one component of magnetic flux density data was proposed. The magnetic field required was created by injecting a current into the imaging object through a single pair of surface electrodes. Then, the modified object function Ψ_K was used for the optimization instead of the usual object function Ψ_U .

We can also express the object function as follows:

$$\Psi_B(\sigma) = \frac{1}{2} \sum \| \mathbf{B}_M - \mathbf{B}_{FEM}(\sigma) \|^2 + \frac{1}{2} \alpha \| \mathbf{L}\sigma \|^2.$$

Here, \mathbf{B}_M , \mathbf{B}_{FEM} are the measured and calculated values of magnetic flux density outside the given object. The algorithm based on the minimization of the object function Ψ_B was also tested. In comparison with the case when the object function Ψ_K is minimized, the quality of obtained reconstruction results was somewhat worse and this technique was more time-consuming.

Finally, the reduction of the number of unknowns (in accordance with a suitable filter based on, for example, the knowledge of conductivity on some elements) was introduced to the forward solution of the basic iteration process.

The applicability of this new feasible algorithm was verified on different numerical examples. The representative results were presented in this paper; they confirm that the proposed algorithm can stably and effectively determine the internal conductivity distribution and also con

ductivity changes in an imaging slice. The new approach is based on the use of magnetic field data, which can be obtained by a wireless measurement. This is the main advantage compared to the EIT approach.

The resolution of new method depends on the density of mesh, namely the number of unknown $\sigma^{(e)}$. Therefore, stability and convergence of the reconstruction process will be ensured, if the number of measured values (voltage or components of magnetic field) is equal to or greater than the number of unknown. Unfortunately, the proposed way is not applicable to 3D image reconstruction of conductivity distribution.

The electrical properties of healthy and ill tissues have been studied for a long time. It is possible to say that e.g. the dielectric properties of the tumor cells showed higher permittivity and conductivity values than a homologous healthy tissue [16]. Further investigation will be therefore focused on the main goal - to introduce in the proposed algorithm the possibility of permittivity image reconstructions.

Acknowledgements

The research described in the paper was financially supported by the research program MSM 0021630513.

References

- [1] HOLDER, D. S. *Electrical Impedance Tomography*. Philadelphia: IOP Publishing, 2005.
- [2] SIKORA, J., WÓJTOWICZ, S. *Industrial and Biological Tomography. Theoretical Basis and Applications*. Warsaw: Electrotechnical Institute, 2010.
- [3] SANKOWSKI, D., SIKORA, J. *Electrical Capacitance Tomography. Theoretical Basis and Applications*. Warsaw: Electrotechnical Institute, 2010.
- [4] CRILE, G. W., HOSMER, H. R., ROWLAND, A. F. The electrical conductivity of animal tissue under normal and pathological conditions. *American Journal of Physiology*, 1922, vol. 60, no. 1, p. 59 - 106.
- [5] MEYER, A. W. Method for detecting brain tumors in the trepanation by electrical resistance measurement (Methode zum Auffinden von Hirntumoren bei der Trepanation durch elektrische Widerstandsmessung). *Zentralblatt für Chirurgie*, 1921, no. 48, p. 1824 - 1826 (in German).
- [6] FOSTER, K. R., SCHWAN, H. P. Dielectric properties of tissues and biological materials: a critical review. *Critical Reviews in Biomedical Engineering*, 1989, vol. 17, no. 1, p. 25 - 104.
- [7] GEDDES, L. A., BAKER, L. E. The specific resistance of biological materials - a compendium of data for the biomedical engineer and physiologist. *Medical and Biological Engineering and Computing*, 1967, vol. 5, no. 3, p. 271 - 293.
- [8] LAW, S. K. Thickness and resistivity variations over the upper surface of the human skull. *Brain Topography*, 1993, vol. 6, no. 2, p. 99 - 109.
- [9] SEO, J. K., KWON, O., WOO, E. J. Magnetic resonance electrical impedance measurement tomography (MREIT): conductivity and current density imaging. *Journal of Physics: Conference Series*, 2005, vol. 12, p. 140 - 155.
- [10] JEON, K., LEE, C.-O., WOO, E. J., KIM, H. J., SEO, J. K. MREIT conductivity imaging based on the local harmonic B_z algorithm: animal experiments. *Journal of Physics: Conference Series*, 2010, vol. 224, no. 1, p. 1 - 4.
- [11] LEE, T. H., NAM, H. S., LEE, M. G., KIM, Y. J., WOO, E. J., KWON, O. I. Reconstruction of conductivity using the dual-loop method with one injection current in MREIT. *Physics in Medicine and Biology*, 2010, vol. 55, no. 24, p. 7523 - 7539.
- [12] KWON, O., LEE, J. Y., YOON, J. R. Equipotential line method for magnetic resonance electrical impedance tomography. *Inverse Problems*, 2002, vol. 18, p. 1-12.
- [13] ZHANG, X., YAN, D., ZHU, S., HE, B. Noninvasive imaging of head-brain conductivity profiles. *IEEE Engineering in Medicine and Biology Magazine*, 2008, vol. 27, no. 5, p. 78 - 83.
- [14] MIKLAVČIČ, D., PAVŠELI, N., HART, F. X. *Electric Properties of Tissues. Wiley Encyclopedia of Biomedical Engineering*. John Wiley & Sons, 2006.
- [15] DĚDKOVÁ, J., OSTANINA, K. Implementation of fuzzy filters in EIT image reconstructions. *Acta Technica ČSAV*, 2011, vol. 56, no. 2, p. 207 - 216.
- [16] GHANNAM, M. M., EL-GEBALY, R. H., GABER, M. H., ALI, F. F. Inhibition of Ehrlich tumor growth in mice by electric interference therapy (in vivo studies). *Electromagnetic Biology and Medicine*, 2002, vol. 21, no. 3, p. 255 - 268.

About Authors ...

Jarmila DĚDKOVÁ was born in Znojmo in 1959. She received her master's degree in Electrical Engineering from Brno University of Technology in 1983. Her professional and current research interests are directed towards the development of algorithms for the electromagnetic field modeling, optimization and effective solution of inverse problems.

Ksenia OSTANINA was born in Izhevsk in 1987. She received her master's degree in Electrical Engineering from Izhevsk State Technical University in 2009. Her research is focused on numerical methods for image reconstructions of biological tissues conductivity.